Biochimica et Biophysica Acta 1812 (2011) 732–742

Contents lists available at ScienceDirect

Biochimica et Biophysica Acta

journal homepage: www.elsevier.com/locate/bbadis

Mis-splicing of Tau exon 10 in myotonic dystrophy type 1 is reproduced by overexpression of CELF2 but not by MBNL1 silencing

C.M. Dhaenens [a,b,1], H. Tran [a,b,1], M.-L. Frandemiche [a,b], C. Carpentier [a,b], S. Schraen-Maschke [a,b,1], A. Sistiaga [c,d,g,1], M. Goicoechea [c,d,g], S. Eddarkaoui [a,b], E. Van Brussels [a,b], H. Obriot [a,b], A. Labudeck [e], M.H. Gevaert [e], F. Fernandez-Gomez [a,b], N. Charlet-Berguerand [f], V. Deramecourt [e], C.A. Maurage [a,b,e], L. Buée [a,b], A. Lopez de Munain [c,d,g,1], B. Sablonnière [a,b], M.L. Caillet-Boudin [a,b], N. Sergeant [a,b,*,1]

[a] Inserm, U837-1, Alzheimer & Tauopathies, place de Verdun, F-59045 Lille, France
[b] Univ Lille Nord de France, UDSL, Faculty of Medicine, Institute of Predictive Medicine and Therapeutic Research, Jean-Pierre Aubert Research Centre, place de Verdun, F-59045 Lille, France
[c] Donostia Hospital, Experimental Unit, Paseo Dr. Begiristain s/n, 20014 San Sebastian, Spain
[d] Centro de Investigación Biomédica en Red sobre Enfermedades Neurodegenerativas (CIBERNED) C/ Valderrebollo, 528031 Madrid, Spain
[e] CHULille, Neuropathological Department, Regional University Hospital Centre, F-59037 Lille, France
[f] Inserm, AVENIR Group, IGBMC, 1 Rue Laurent FRIES, 67404 Illkrich, France
[g] Donostia Hospital, Neurological Unit, Po Dr Begiristain s/n, 20014 San Sebastian, Spain

ARTICLE INFO

Article history:
Received 18 June 2010
Received in revised form 16 March 2011
Accepted 17 March 2011
Available online 23 March 2011

Keywords:
Myotonic dystrophy
Triplet expansion disease
Microtubule-associated protein Tau
Splicing
CELF splicing factor family
MBNL1

ABSTRACT

Tau is the proteinaceous component of intraneuronal aggregates common to neurodegenerative diseases called Tauopathies, including myotonic dystrophy type 1. In myotonic dystrophy type 1, the presence of microtubule-associated protein Tau aggregates is associated with a mis-splicing of Tau. A toxic gain-of-function at the ribonucleic acid level is a major etiological factor responsible for the mis-splicing of several transcripts in myotonic dystrophy type 1. These are probably the consequence of a loss of muscleblind-like 1 (MBNL1) function or gain of CUGBP1 and ETR3-like factor 1 (CELF1) splicing function. Whether these two dysfunctions occur together or separately and whether all mis-splicing events in myotonic dystrophy type 1 brain result from one or both of these dysfunctions remains unknown. Here, we analyzed the splicing of Tau exons 2 and 10 in the brain of myotonic dystrophy type 1 patients. Two myotonic dystrophy type 1 patients showed a mis-splicing of exon 10 whereas exon 2-inclusion was reduced in all myotonic dystrophy type 1 patients. In order to determine the potential factors responsible for exon 10 mis-splicing, we studied the effect of the splicing factors muscleblind-like 1 (MBNL1), CUGBP1 and ETR3-like factor 1 (CELF1), CUGBP1 and ETR3-like factor 2 (CELF2), and CUGBP1 and ETR3-like factor 4 (CELF4) or a dominant-negative CUGBP1 and ETR-3 like factor (CELF) factor on Tau exon 10 splicing by ectopic expression or siRNA. Interestingly, the inclusion of Tau exon 10 is reduced by CUGBP1 and ETR3-like factor 2 (CELF2) whereas it is insensitive to the loss-of-function of muscleblind-like 1 (MBNL1), CUGBP1 and ETR3-like factor 1 (CELF1) gain-of-function, or a dominant-negative of CUGBP1 and ETR-3 like factor (CELF) factor. Moreover, we observed an increased expression of CUGBP1 and ETR3-like factor 2 (CELF2) only in the brain of myotonic dystrophy type 1 patients with a mis-splicing of exon 10. Taken together, our results indicate the occurrence of a mis-splicing event in myotonic dystrophy type 1 that is induced neither by a loss of muscleblind-like 1 (MBNL1) function nor by a gain of CUGBP1 and ETR3-like factor 1 (CELF1) function but is rather associated to CUGBP1 and ETR3-like factor 2 (CELF2) gain-of-function.

1. Introduction

Myotonic dystrophy type 1 (Steinert's disease) is an inherited neuromuscular disease affecting multiple organs, including skeletal and smooth muscle (myotonia), the heart (arrhythmias, conduction defects), the endocrine system (hyperinsulinemia), and the eyes (cataracts) [1]. The involvement of the central nervous system in DM1 was reported long ago [2,3], but systematic studies to analyze the brain structures and cognitive functions involved have only recently been initiated. The available clinical data suggest that patients experience focused executive and visuoconstructive difficulties [4–7] and frontal cognitive impairment including attentional ability worsening with aging [8,9]. In addition, impairments in facial emotion recognition have been associated with the adult form of DM1 [5]. These clinical findings suggest the involvement of the cerebral cortex as well as subcortical areas, such as the amygdala. In line with these

* Corresponding author at: Inserm U837-1, Alzheimer & Tauopathies, Univ Lille Nord de France, USDL, IMPRT, Batiment Biserte, 1, place de Verdun, rue Polonowski, F-59045 Lille, France.
E-mail address: nicolas.sergeant@inserm.fr (N. Sergeant).
[1] Equal contribution to the work.

0925-4439/$ – see front matter © 2011 Elsevier B.V. All rights reserved.
doi:10.1016/j.bbadis.2011.03.010

observations, biomarkers of Alzheimer's disease including amyloid-beta peptide and Tau protein concentrations in the cerebrospinal fluid were shown to be significantly reduced and increased, respectively, in DM1 when compared to aged-matched control patients [10]. Structural neuroimaging in DM1 patients reveals the presence of brain atrophy and white matter lesions [11–13].

At the neuropathological level, neurofibrillary tangles (NFTs) are found in the limbic system of DM1 patients, including the hippocampus and isocortical areas such as the temporal and frontal cortices [14–16]. NFTs are intraneuronal aggregates made of hyper- and abnormally phosphorylated isoforms of microtubule-associated Tau (for review, see reference 17). Tau proteins belong to the family of microtubule-associated proteins and are encoded by a single *MAPT* gene located on chromosome 17. The alternative splicing of Tau exons 2, 3, and 10 gives rise to 6 adult human brain isoforms that are principally expressed in neurons and localized preferentially in the axons. The alternative splicing of Tau is developmentally regulated, tissue specific, and deregulated in several Tauopathies [18]. In frontotemporal dementia, *MAPT* gene mutations modify the splicing of Tau, leading to the development of NFTs in adulthood. In DM1, we reported a modified splicing pattern for Tau, essentially characterized by the reduced inclusion of exons 2 and 3 [15,19]. A reduction in the inclusion of Tau exon 10 has also been reported in several brains from DM1 patients [20] as well as in a transgenic animal model of DM1 [21]. However, the molecular mechanism underlying the mis-splicing of exon 10 in DM1 and its functional consequences remain unknown. This is of importance since the Tau exon 10 encodes for a fourth microtubule-binding domain. Thus, Tau proteins with four microtubule-binding domains (4R) bind more avidly and further stabilize microtubules than those with three binding domains (3R). The increased expression of 3R Tau isoforms in DM1 may modify the axonal transport and plasticity since Tau is suggested to regulate the motor protein transport along microtubules [22]. Moreover, a growing body of evidences suggests that Tau proteins may also localize to spines of dendrites and regulate glutamatergic transmission [23,24]. The splicing of N-methyl D-aspartate receptor subunit one is altered in DM1 brains [19,20], which, together with the mis-splicing of Tau, may also deregulate the glutamatergic synaptic transmission. Thus, the reduced Tau protein isoforms expressed in DM1 brains and the development of NFT may contribute to the cognitive impairments in DM1.

A toxic gain-of-function at the RNA level is the main pathophysiological hypothesis to explain the development of the disease. DM1 is a genetically inherited disease characterized by a dynamic and unstable trinucleotide repeat expansion in the 3′ UTR of the *DMPK* gene [25]. DMPK transcripts bearing long CUG repeats are retained in the nucleus and accumulate to form ribonuclear protein inclusions called foci. This nuclear retention of mutated transcripts of DMPK is responsible for DMPK haploinsufficiency. In addition, the sequestration inside foci of proteins such as members of the MBNL family of splicing factors results in a partial loss-of-function of these splicing factors [26,27]. Moreover, a gain-of-function of CUG-binding protein and Elav-type RNA binding protein 3 (ETR3)-like factor 1 (CUG-binding protein 1 (CUGBP1)/CELF1) in skeletal or heart muscle, through its stabilization and phosphorylation by PKC, is also instrumental to DM1 pathophysiology [28–30]. CELF1 and embryonic lethal abnormal vision-like RNA-binding protein-3 (ETR3/CELF2) like factors (CELF) belong to a family of RNA-binding proteins that includes 6 members. While both CELF1 and CELF2 are ubiquitously expressed, the latter is highly expressed in the brain and heart of rodents [31,32]. The four other members, CELF3, 4, 5, and 6, are enriched in the rodent brain. However, less is known about their expression in the human brain and their potential implication in DM1.

Dysfunctions of MBNL1 and CELF1 together are responsible for the modified splicing of several transcripts in DM1 muscle. However, whether the two dysfunctions occur concomitantly or separately and whether CELF family members other than CELF1 are involved in DM1 brain remain to be determined. We previously suggested that a loss of MBNL1 or a gain of CELF2 function could repress Tau exon 2-inclusion as observed in human disease [19,33]. In the present study, we extended our analysis to additional DM1 patients, and observed that, in addition to the presence of NFTs in all DM1 patients, certain patients displayed a mis-splicing of exon 10 in addition to that of exon 2. We therefore investigated the factors potentially responsible for this difference between patients as well as the mechanism involved in the deregulation of Tau exon 10 splicing.

2. Results

2.1. Clinical and genetic presentation

In the present study, we first analyzed the presence of *DMPK* CTG-expansions, the brain distribution of NFTs, and Tau protein expression in the brain tissue of two new DM1 patients (DM1a and DM1e) in order to determine whether their phenotype was comparable to that of the DM1 patients previously described [15]. Using small pool PCR with 0.5 ng of DNA, we have observed CTG-expansion in 5 brain regions in DM1a (Fig. 1A, left panel) and 6 regions in DM1e (Fig. 1A, right panel). The smaller expanded allele of patient DM1a, visible in the hippocampus and frontal and entorhinal cortices, was of 150 CTG (Fig. 1A, left panel) and likely corresponds to the progenitor mutant allele. The largest allele of patient DM1e, seen in the hippocampus, contained 2900 CTG repeats, but several alleles with more than 1500 CTG repeats were observed in the other brain regions (Fig. 1A, right panel). However, the number of expanded alleles detected is well below that expected relative to the quantity of input DNA. The number of expanded alleles and CTG repeat lengths were comparable to those observed in the DM1 patients studied previously [15]. However, these data suggest that a high proportion of brain cells may contain alleles too large to be efficiently amplified by PCR, resulting in a probable underestimation of the true level of diversity within each sample.

2.2. Brain distribution of NFTs and Tau isoform expression

In order to analyze Tau pathology and its topographic distribution in the brain of DM1a and DM1e, the presence or absence of NFTs was established in several brain regions, including the entorhinal, the hippocampus, the amygdala, the basal and dorsolateral frontal, the parietal and the occipital cortices, using immunohistochemistry (Fig. 1B). NFTs composed of hyperphosphorylated Tau could be seen using phospho-specific AT8, AD2, AT100, and S199P antibodies and a pan TauCter antibody. Similar staining was observed in the amygdala and hippocampus of patient DM1e (not shown). The immunohistochemical observations were correlated with Western blotting studies of Tau pathology. Using the phospho-specific Tau antibody AD2, we observed the typical pathological Tau quartet of 60, 64, 69, and 74 kDa in the sample from an Alzheimer's disease (AD) patient (Fig. 1C, lanes 1 and 2). Tau proteins were not detected using the AD2 antibody in control brain tissue (Fig. 1C and S1A, lanes 3 and 2, respectively). Pathological Tau proteins were detected and consisted of 2 bands of 60 and 64 kDa in the hippocampus (Fig. 1C, lane 5) and temporal amygdala (Fig. 1C, lane 6) and a single band of 60 kDa in the entorhinal cortex (Fig. 1C, lane 4) of DM1a, the insula, and temporal pole of DM1e (Fig. S1A, lanes 3–6). We next used an antibody to the N-terminus of Tau (TauNter) to analyze the overall expression of Tau protein isoforms. Full-length Tau isoforms in the adult brain were resolved as four bands in the control case (Fig 1C, lane 3; Fig. S1A, lane 2, dots). The bands under the full-length isoforms correspond to catabolic products. In all brain regions studied in both DM1a and DM1e, 2 main bands were detected at 55 and 60 kDa, whereas the 64 kDa Tau band was faintly labeled, and the upper bands were not detected (Fig. 1C and Fig. S1A). In order to determine the Tau isoforms expressed in DM1

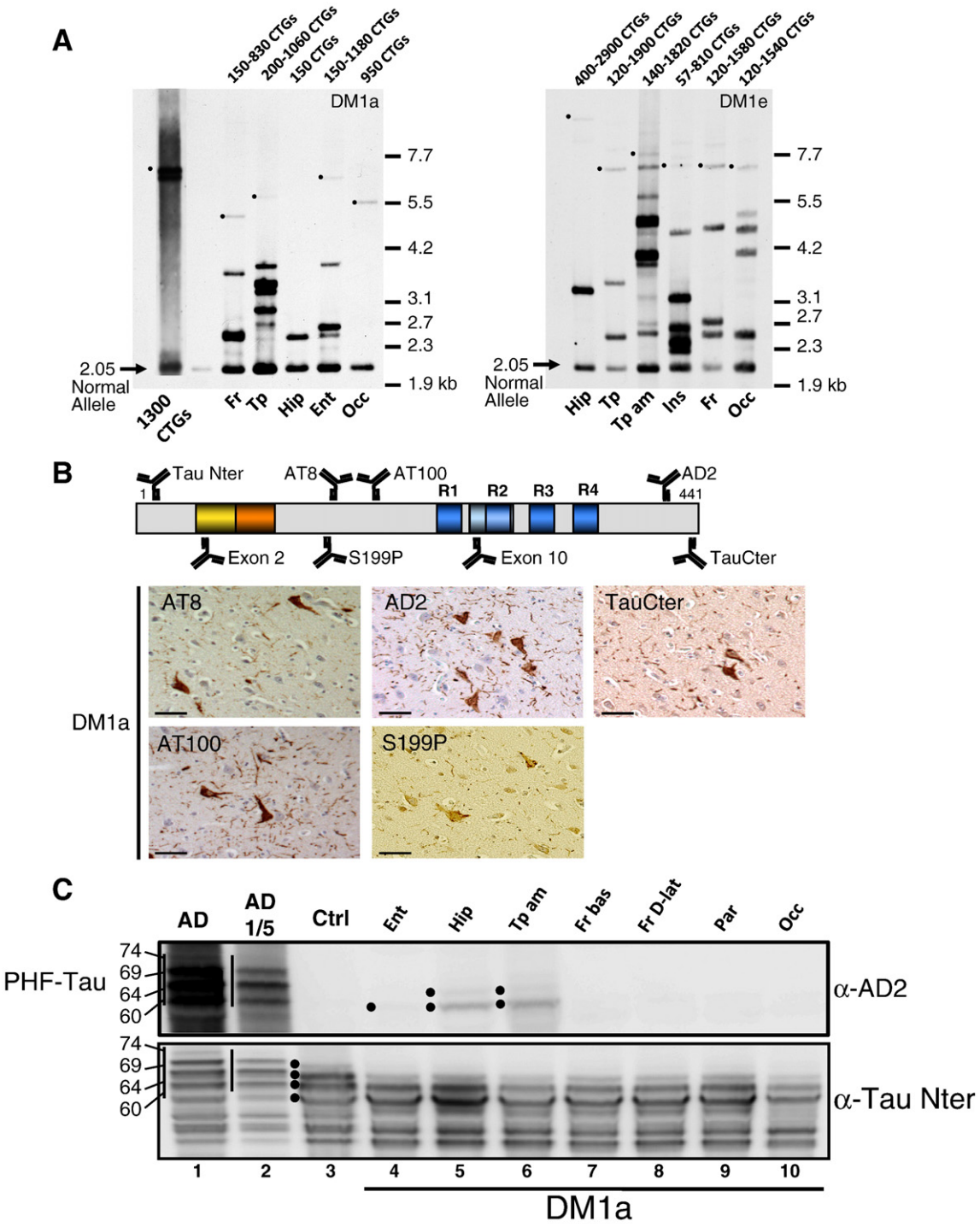

Fig. 1. CTG expansion mosaicism, neurofibrillary degeneration, and Tau protein expression in DM1 brain tissue. A) CTG repeat lengths were determined from the genomic DNA of cortical (frontal (Fr), temporal (Tp), amygdala (Tp am), insula (Ins), hippocampus (Hip), entorhinal (Ent), and occipital (Occ)) brain tissues of DM1a and DM1e using long PCR followed by Southern blotting for expanded alleles. Results are shown for 0.5 ng of input DNA. Lane 1 (DM1a panel) corresponds to expanded control DNA (1300 CTG repeats) from a congenital form of DM1. DNA molecular weight markers are indicated on the right. Dots indicate the longest expanded alleles for each brain region analyzed. B) Top: location of epitopes recognized by the antibodies used with respect to the longest brain Tau isoform (441 aa isoform). Bottom: neurofibrillary tangles (NFTs) in the amygdala of DM1a. NFTs composed of abnormal and hyperphosphorylated Tau are stained by AT8, AD2, TauCter, AT100, and S199P antibodies. C) Spatial distribution of hyperphosphorylated Tau (PHF-Tau) in DM1a brain. Using the phospho-specific Tau antibody AD2, hyperphosphorylated Tau isoforms (PHF-Tau) were detected only in brain regions with NFTs. Seven cortical brain regions of DM1a (lanes 4 to 10: entorhinal (Ent), hippocampus (Hip), temporal amygdala (Tp am), basal frontal (Fr bas), dorsolateral frontal (Fr D-lat), parietal (Par), and occipital (Occ)) were analyzed by Western blotting using a Tau N-terminal antibody to detect all isoforms and compared to the frontal cortex of an Alzheimer's disease patient (lane 1 and 2) and to the same region of a control individual (lane 3). In the control brain, Tau isoforms were detected as 4 bands between 50 and 67 kDa (black dots). Note that the bands under the 60 kDa Tau band detected with antibody TauNter correspond to amino-terminal catabolic products of Tau protein isoforms. The vertical bar indicates the position of the pathological Tau protein quartet in lanes 1 and 2.

brains, we used Tau exon-specific antibodies (Fig. S1B). In the control case, 3 bands (55, 60, 64 kDa) corresponding to full-length Tau isoforms were detected using an antibody to Tau isoforms lacking exon 10 (Fig. S1B, panel Exon 10−). In contrast, the exon 10-specific antibody stained strongly the 60 kDa band and, to a lesser extent, the bands at 55 and 64 kDa (Fig. S1B, panel Exon 10+, lane Ctrl). The exon

2-specific antibody stained the 55 and 60 kDa bands and, to a lesser extent, the 64 kDa band. In both DM1a and DM1e, there was a strong reduction of Tau isoforms stained with antibodies specific to exons 10 and 2 (Fig. S1B, panels Exon 10+ and Exon 2+), suggesting an alteration in Tau protein isoform expression. We next determined the composition of the Tau isoforms found in NFTs by immunohistochemistry, using Tau antibodies specific to exons 2 and 10 (Fig. S1C). As a positive control, NFTs in an AD brain were stained with the AD2 phospho-Tau antibody as well as with Tau exon-specific antibodies (Fig. S1C). In sharp contrast, in serial sections of the amygdala of patient DM1a, no NFTs or neuropil threads were detected with exon-specific Tau antibodies (Fig. S1C). This result suggests that no other isoforms than those lacking exons 2 and 10 are found in NFTs of DM1 brains.

2.3. Tau splicing modification in DM1 patients

Immunohistochemical and Western blot analyses indicate a modified expression of Tau protein isoforms in the brain of patients DM1a and DM1e, including the loss of Tau isoforms containing the sequence encoded by exon 10. We therefore analyzed Tau isoform expression at the mRNA level in five brain regions in comparison with previously studied DM1 patients (Fig. 2 and Fig. S2). With regard to Tau exon 2/3 splicing, in the control brain, exon 2 was included in 53% ± 1% of Tau transcripts (Fig. 2A, histogram). In the brain of DM1a and DM1e, this proportion significantly dropped to 35% ± 3% ($p = 0.0079$) and 31% ± 2% ($p < 0.0001$), respectively, demonstrating a preferential skipping of exon 2 (Fig. 2, histogram). To estimate Tau exon 10-inclusion, primers in exons 9 and 11 were used. The splicing of exon 10 was measured in the hippocampus, temporal, parietal entorhinal, and frontal cortices of a control, DM1a, and DM1e patients (Fig. S2). On average, the percentage of Tau exon 10 inclusion in the control brain regions was of 47% ± 2%, consistent with the fact that half of the 6 Tau isoforms contain exon 10. On average, in both DM1a and DM1e, a reduced inclusion of exon 10 was observed when compared to the control (DM1a, 23% ± 4%; DM1e, 31% ± 2%). Apart from the parietal cortex of DM1a, the reduced inclusion of exon 10 was similar between brain regions analyzed. We further compared the splicing pattern of exon 10 in the temporal cortex between 4 controls and 5 DM1 brains at our disposal. In the temporal cortex of the 4 controls, the percentage of Tau exon 10-inclusion was of 46.5% ± 1.5% and homogeneous. In DM1a, there was a significant reduction of Tau exon 10-inclusion to 37% ± 3% ($p = 0.0013$) (Fig. 2B). Tau exon 10-inclusion was also reduced in the brain of DM1e (38% ± 2%; $p = 0.002$). In contrast, this reduction was not observed in DM1b, c, and d. Thus, the modified splicing of Tau exon 2 is a robust and common phenotype in all DM1 brains analyzed so far, and it is also homogenous among brain areas. In contrast, the reduced inclusion of exon 10 is less pronounced and not constant in DM1 patients. One of the possible factors known to influence Tau exon 10 splicing is *MAPT* gene haplotype (H1 or H2), which has been suggested to modify the level of exon 10-inclusion [34]. Thus, we genotyped all patients included in the present study. DM1 patients were all H1/H1 (data not shown), excluding the possibility that variation of Tau exon 10 splicing could have been related to polymorphisms of *MAPT* gene haplotype.

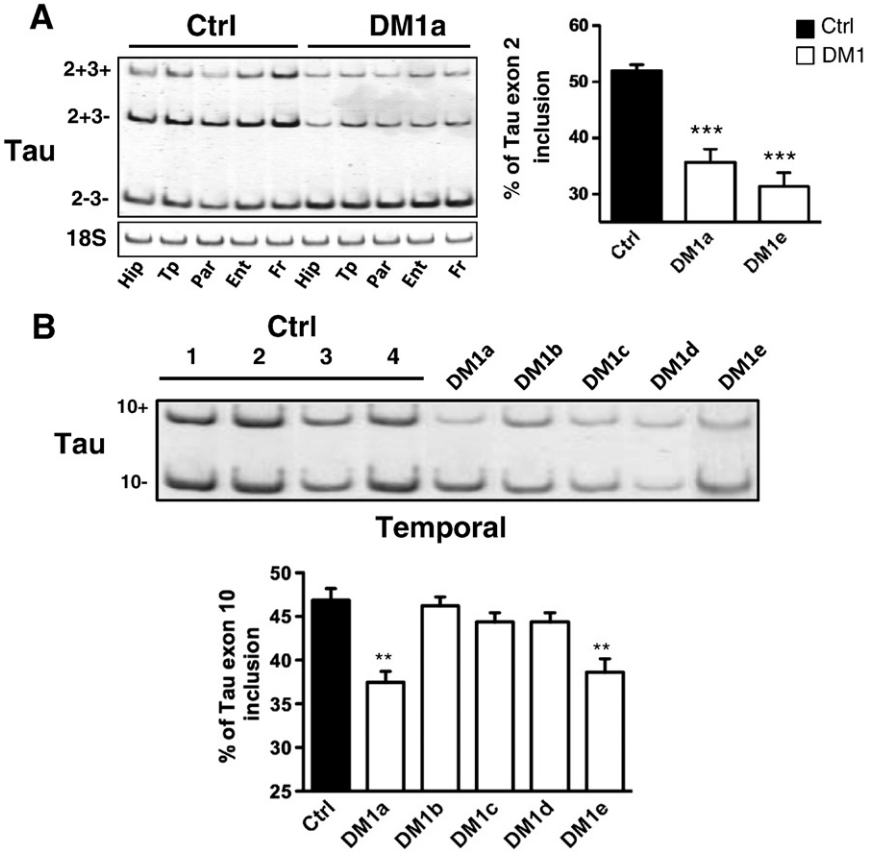

Fig. 2. Tau splicing in controls and DM1 patients. A) Exclusion of Tau exon 2 in the brain of DM1a and DM1e. Left panel (DM1e not shown): Tau exon 2/3 forward and reverse primers allowed the simultaneous amplification of Tau isoforms with exons 2 and 3 (2+3+), with exon 2 but not 3 (2+3−), or lacking both exons (2−3−). PCR was performed using samples from the hippocampus (Hip), temporal (Tp), parietal (Par), entorhinal (Ent), and frontal (Fr) cortical brain regions of a control individual and patient DM1a. 18S RNA was used as the internal loading standard. Right panel: histogram showing the percentage of transcripts containing exon 2 in the brain of DM1a and DM1e. The mean and standard deviation were calculated from three individual RT–PCR experiments resulting from the study of four brain regions of two controls (in black) and patients DM1a and DM1e (in white). ***$p < 0.0001$. B) Tau exon 10 splicing in DM1 brain. RT–PCR analyses of Tau exon 10 inclusion in the temporal cortex of 4 controls and 5 DM1 patients. Histograms indicate the percentage of transcripts including exon 10, from 3 independent experiments. Tau exon 10 inclusion is significantly reduced in DM1a and DM1e but not in DM1b, c, or d. **$p < 0.01$.

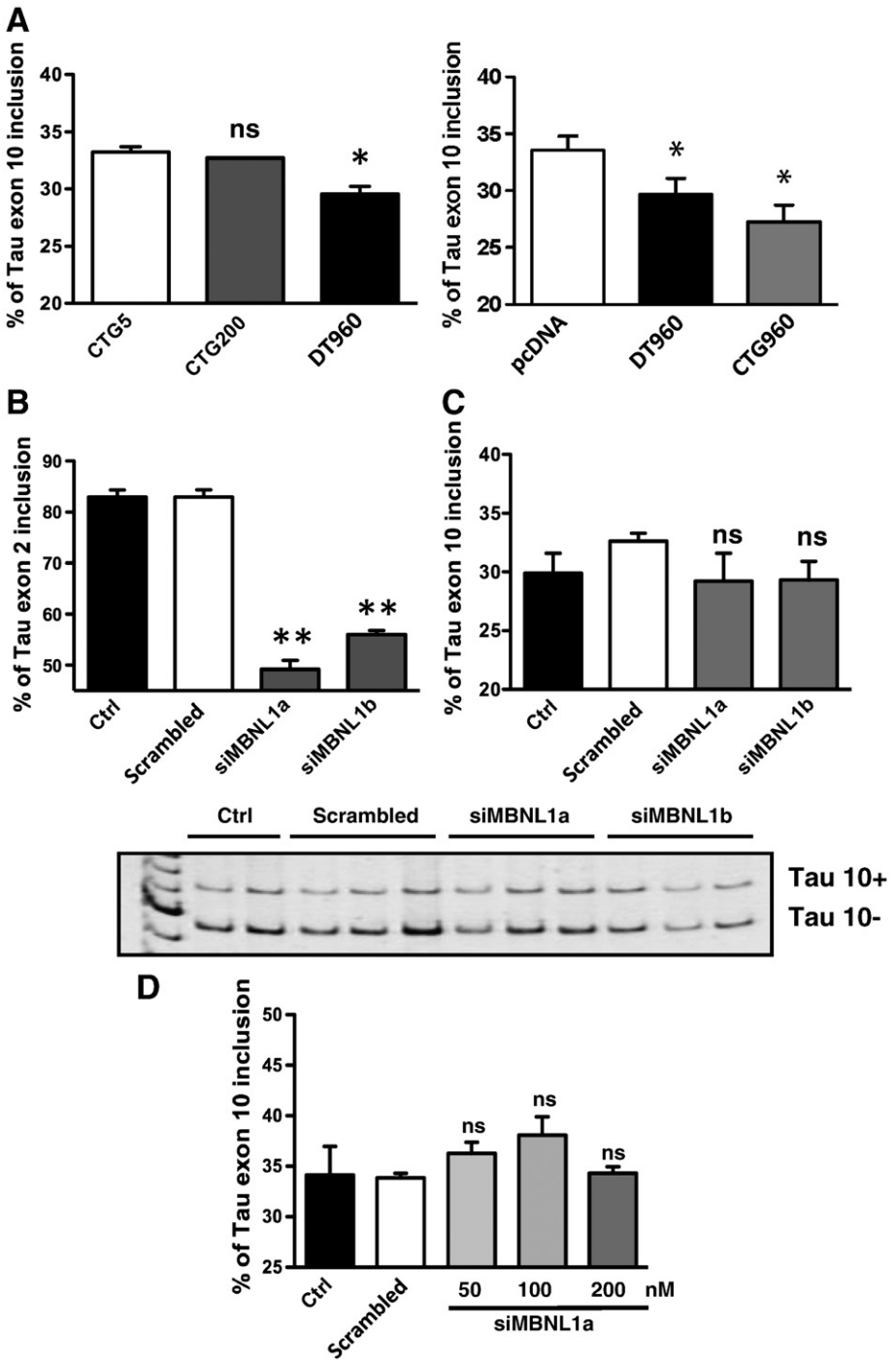

Fig. 3. Effect of long CTG repeats and MBNL1 loss-of-function on Tau splicing. A) Overexpression of long CUG repeats in HeLa cells mimics the Tau exon 10-exclusion observed in the brain of DM1a and DM1e. The 3′ UTR of the human *DMPK* (1 μg) containing 5 (CTG5), 200 (CTG200), or 960 CTG (DT960), subcloned in a pcDNA3.1 plasmid, were transiently transfected in HeLa cells (left panel). HeLa were also transfected with empty pcDNA 3.1 plasmid DT960 and CTG960 vector, which lacks *DMPK* exons 11 to 14 and only contains the CTG repeats (right panel). Total RNA was isolated 48 h post-transfection. Primers Tau exon 10 forward and reverse allowed the simultaneous amplification of Tau isoforms with or without exon 10. 18S RNA was used as the internal loading standard. After polyacrylamide gel electrophoresis, bands were quantified and results are expressed as the percentage of Tau exon 10 inclusion. Histogram represents the mean ± SEM of four individual experiments. $^{*}p<0.05$; ns indicates non-significant; Mann–Whitney *U* test. B) Loss of MBNL1 expression reduces Tau exon 2-inclusion. The histogram is representative of 3 individual experiments and values are expressed as mean ± SEM. $^{**}p<0.01$. C) Tau exon 10 splicing is insensitive to MBNL1 loss of expression using siRNA. The PCR gel represents the results obtained with two RNA duplexes targeting human MBNL1, siMBNL1a (lanes 6–8) and siMBNL1b (lanes 9–11), and one scrambled duplex (siMBNL1 Scr, lanes 3–5) that were used for transfection into HeLa cells. Lanes 1–2: control (Ctrl), transfection agent alone. ns indicates non-significant; Mann–Whitney *U* test. Means and standard deviations were calculated for 3 individual experiments. D) Evaluation of incremental concentrations (siMBNL1 50, 100, and 200 nM) of siMBNL1a upon Tau exon 10 splicing. The histogram represents the average ± SEM of percentage of Tau exon 10-inclusion obtained from 3 independent experiments (ns indicates non-significant).

2.4. DMPK CTG repeats reduce Tau exon 10 inclusion

The effect of *DMPK* long CTG repeats on Tau exon 10 splicing was next investigated (Fig. 3A). Tau exon 10 splicing is developmentally regulated—the switch between exclusion and inclusion of exon 10 is postnatal. Here, we used HeLa cells or T98 glioblastoma cells to analyze the trans-dominant effect of long CUG repeats because, opposite to neuroblastoma cell-line SY5Y, exon 10 is alternatively

spliced in HeLa and T98 but completely excluded in SY5Y [33]. Under control conditions, exon 10 was included in 33% ± 0.5% and 36% ± 2% of HeLa and T98 Tau transcripts, respectively (Fig. 3A and S3A). We transfected HeLa and T98 with CTG_5, CTG_{200}, and DT_{960} constructs, all under the same CMV promoter. The splicing of exon 10 was not significantly modified by CTG_5 or CTG_{200} whereas it was moderately but significantly reduced to 29.5% ± 0.5% ($p<0.05$) by DT_{960} in both HeLa and T98 cells (Fig. 3A and S3A). The splicing of exon 10 was similarly modified by CTG_{960} lacking the preceding *DMPK* exons 11 to 14, which are present in DT960 construct (Fig. 3A and S3B), or remained unchanged with the *DMPK* 3′ UTR lacking the mutated allele (data not shown). Modification of Tau exon 10 splicing was not related to the presence or absence of DMPK exons. Moreover, despite the differences observed among patients, Tau exon 10 splicing shares the same sensitivity towards long CUG repeats as other cerebral transcripts.

2.5. Differential effect of MBNL1 and CELF proteins on Tau splicing

The loss-of-function of MBNL1 is instrumental in the pathophysiology of DM1 due to its sequestration into ribonucleoprotein aggregates. As shown in Fig. 3B, the inactivation of MBNL1 expression with two siRNA duplexes—siMBNL1a and siMBNL1b—significantly reduced the inclusion of Tau exon 2, attesting the efficacy of siRNA duplexes. Incremental doses from 50 to 200 nM of siMBNL1a duplex were also evaluated and the repression of Tau exon 2-inclusion was already observed at 50 nM (Fig. S3C). However, MBNL1 siRNA did not significantly modify the inclusion of Tau exon 10, regardless of the duplex used (Fig. 3C, histogram and PCR) or the concentration used (Fig. 3D and S3D).

The CELF family also plays a role in DM1 pathophysiology. Moreover, we previously demonstrated the repressive role of CELF2 and CELF4 proteins in Tau exon 2-inclusion [33]. Moreover, CELF3 and CELF4 splicing factors promote the inclusion of Tau exon 10 [18,35]. However, we do not know whether Tau exon 10 splicing is sensitive to CELF1 or CELF2 splicing factors. We therefore analyzed the effect of CELF1, CELF2, or CELF4 overexpression on the splicing of Tau exons 2 and 10. For siRNA experiments, two independent CELF1 siRNA were tested and incremental concentrations were evaluated (Fig. S4A and B). CELF1 mRNA and protein expression were more strongly reduced by siCELFa than with siCELFb (Fig. S4A). The former was therefore selected for the subsequent experiments. Neither CELF1 overexpression (Fig. 4A) nor silencing (Fig. S4C and D) had an effect upon the splicing of Tau exons 2 and 10. In contrast, CELF2 and CELF4 significantly reduced Tau exon 2-inclusion by 17% ($p=0.0001$) and by 12% ($p=0.0012$), respectively (Fig. 4B and C). Interestingly, we observed opposing effects of CELF2 and CELF4 on Tau exon 10 splicing. The overexpression of CELF2 significantly reduced exon 10-inclusion from 37.5% to 31.7% ($p=0.0031$) (Fig. 4B), whereas CELF4 promoted the inclusion of exon 10 by 8% ($p=0.044$; Fig. 4C). CELF4 was described previously as an enhancer of Tau exon 10-inclusion [36]. To exclude a potential artifactual effect due to the efficacy of the vectors or cell-type used, we co-transfected CELF1, CELF2, or CELF4 with the hcTNT exon 5-minigene or a dominant-negative CELF vector (DN-CELF) and reproduced the experiments using both HeLa and T98 cells (Fig. S5B and C). All CELF proteins were expressed as assessed by Western blotting using a V5-epitope antibody for CELF1, 2, and 4 factors or Xpress-epitope antibody for the DN-CELF factor (Fig. S5A). All CELF factors except the DN-CELF promoted the inclusion of exon 5, as previously demonstrated [37] in both HeLa and T98 cells (Fig. S5B and C). Finally, Tau exon-10 inclusion was promoted by CELF4 and repressed by CELF2 but neither by CELF1 nor DN-CELF in both T98 and HeLa cells (Fig. S6).

As several CELF family members appear to be modulators of Tau exon 10 splicing, we finally analyzed the expression of CELF1, CELF2, and CELF4 in brain tissues of DM1 patients as compared to controls (Fig. 5). CELF1, CELF2, and CELF4 were more strongly detected in the temporal, parietal, and frontal cortices of DM1a and DM1e than in samples from the control or patients DM1b, c, or d (Fig. 5A, B, and C). In sharp contrast, in the three latter cases, while CELF4 levels were similar to those observed in the control, CELF2 and CELF1 levels were diminished.

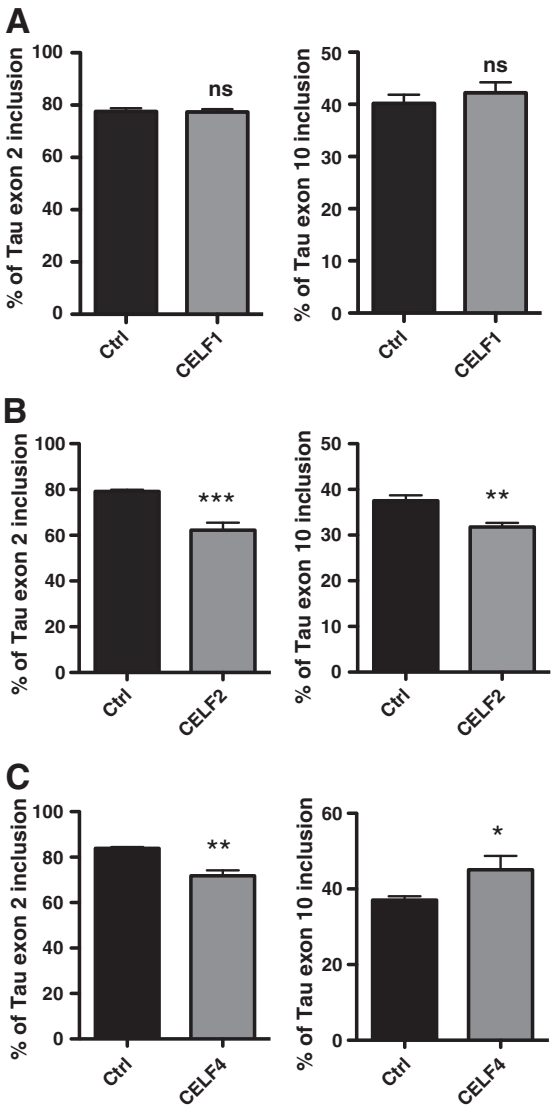

Fig. 4. CELF2 and CELF4, but not CELF1, regulate Tau exon 2 and Tau exon 10 splicing. A) CELF1 expression has no effect on Tau exon 2 and Tau exon 10 splicing (means ± SEM of 4 independent experiments performed in triplicate). Histograms indicate the percentage of Tau exon 2 and exon 10-inclusion in controls (Ctrl) and in HeLa cells ectopically expressing CELF1. ns indicates non-significant; Mann–Whitney *U* test. B) Overexpression of CELF2 reduces the inclusion of Tau exons 2 and 10 (means ± SEM of 5 independent experiments performed in triplicate). $^{**}p<0.001$, $^{***}p<0.0001$, Mann–Whitney *U* test. C) Overexpression of CELF4 decreases Tau exon 2-inclusion and increases Tau exon 10-inclusion (means ± SEM of 4 independent experiments performed in triplicate). $^{**}p<0.001$, Mann–Whitney *U* test. The control experiments correspond to the transfection of the pcDNA 3.1 vector.

3. Discussion

Our data together suggest that the reduced inclusion of Tau exon 10 is not a ubiquitous splicing event in DM1 brains and is probably not related to a loss of MBNL1 or gain of CELF1 functions but rather to a gain of CELF2 function, shown herein to repress Tau exon 10 inclusion. Moreover, the loss of MBNL1 function and gain of CELF function, as far as the brain is concerned, can occur simultaneously or individually and may explain the discrepancies observed in splicing events such as Tau exon 10 splicing.

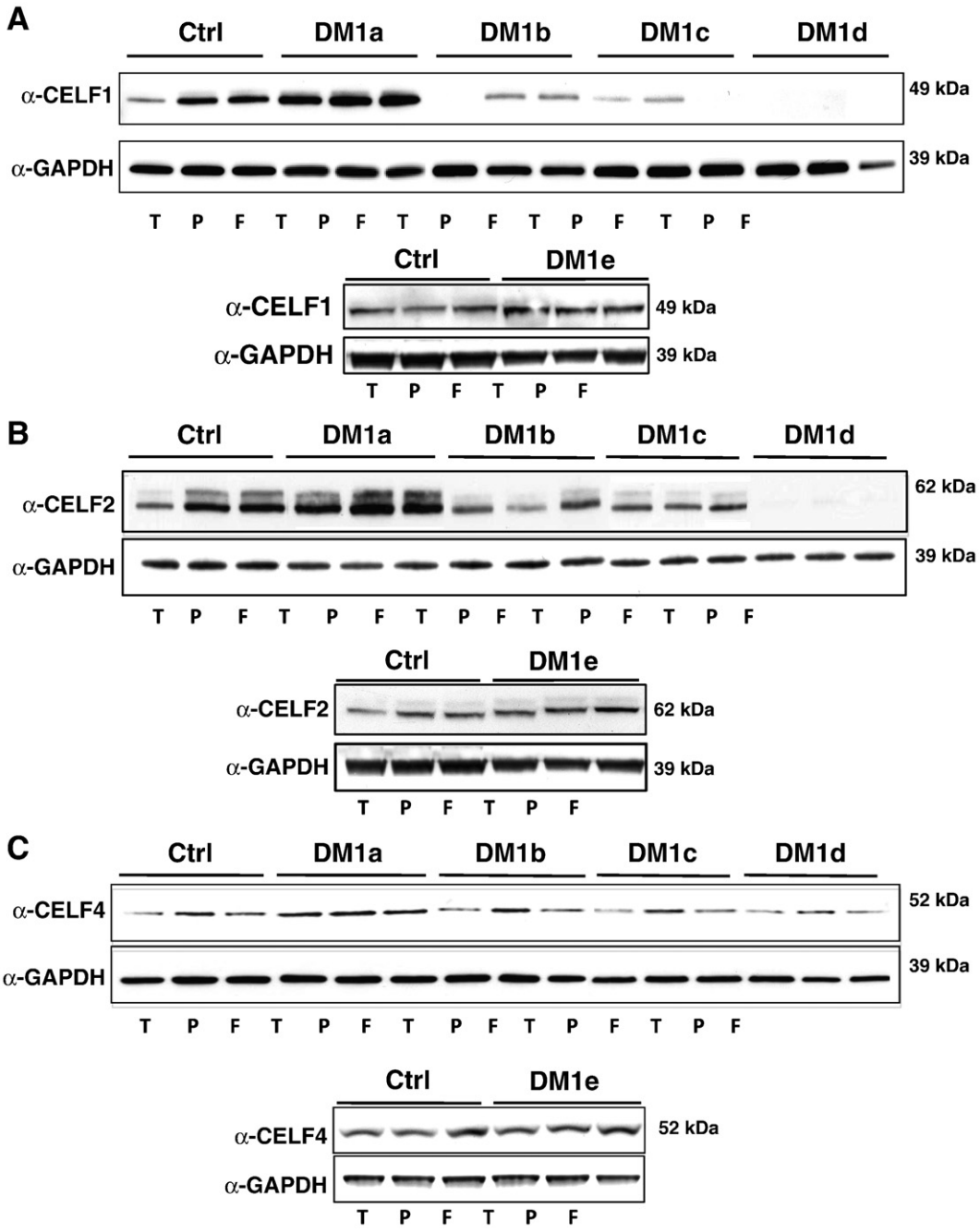

Fig. 5. CELF protein expression in brain tissues. Western blots revealing an overexpression of CELF1 (A) and CELF2 (B) proteins in DM1a and DM1e, using brain tissue lysates from the temporal (T), parietal (P), and frontal cortices (F) of a control individual and patients DM1a, b, c, d, and e. Membranes were stripped and probed with a GAPDH antibody for standardization.

3.1. Presentation of cases with classic DM1 neuropathology but with moderate symptoms

In this study, we described the topographical distribution of NFTs in two patients. These patients presented with a classic adult form of DM1. DM1a was diagnosed at 46 years and displayed muscular abnormalities and early-onset bilateral cataract. He had no cardiac or endocrine disorders nor any cognitive impairment from a clinical point of view. The only neurological symptom reported was diurnal somnolence. The anamnesis was marked by frequent gastrointestinal disorders leading to a grade 3 adenocarcinoma of the colon, which was the cause of death. DM1e was diagnosed at the age of 45 years and had a round, myopathic face; myotonia of both hands; type II diabetes; hypercholesterolemia; and suffered from obesity. Although we do not know the cognitive status of these patients, the topographical distribution of NFTs was very similar to that of DM1 patients already characterized [15]. In our DM1 cohort, we show that Tau pathology is observed early in adulthood and that the hippocampus and temporal cortex, as well as the amygdala and insula, are the most vulnerable regions affected in DM1. Importantly, the amygdala is the brain region controlling fear and facial emotion recognition. In DM1, the latter cognitive function is altered [5]. Moreover, brain imaging also points to the temporo-insular region as a vulnerable brain area [11,38].

3.2. Analysis of splicing modifications in DM1 brains

Although the presence of NFTs is restricted to the hippocampus and temporal amygdala in our study, Tau splicing is altered in all

regions analyzed, suggesting that NFTs only affect a subset of neuronal populations, as observed in other Tauopathies [17,39,40]. Our results show that all DM1 patients, in all brain regions and regardless of the size of the expansion, present a reduction in the inclusion of Tau exon 2. In addition, we were able to confirm a similar ubiquitous increase in the expression of the APP fetal splice variant lacking exons 7 and 8, an increase in the inclusion of NMDAR1 exon 5 [20], and an increase in the expression of the longest MBNL1 isoform, $MBNL1_{43}$ [19] (not shown). In contrast to these splicing mechanisms, we found that Tau exon 10 skipping is not a consistent feature of DM1. Indeed, only 2 among 6 patients presented an abnormal inclusion of Tau exon 10. The 10 DM1 patients previously investigated by Jiang et al. also displayed Tau exon 10 mis-splicing [20]. *MAPT* polymorphism has been reported to influence Tau expression and splicing. In fact, H1 carriers have an increased susceptibility to neurodegeneration, and the H1 chromosome results in higher levels of exon 10+ MAPT mRNA than H2 [34]. We systematically genotype all patients in our cohort, and all our cases—DM1 and controls—were H1/H1. Moreover, the *MAPT* gene between exon 9 and exon 10 was sequenced in DM1a and DM1b to exclude any unknown polymorphism. Thus, even if NFTs were observed, the *MAPT* haplotype could not explain the differential inclusion of exon 10 in DM1 patients. However, exon 10 splicing is sensitive to the identity of its flanking exons. Indeed, exon 9 promotes skipping whereas exon 11 is repressive [36,41].

The mechanism underlying the mis-splicing of Tau exon 10 in DM1 remains completely ill-defined. An alternative explanation, that exon 10 mis-splicing is not directly related to CTG expression, can be ruled out. *In vitro* experiments using long CUG tracts lead to a modification in Tau exon 10 splicing, as observed in the human brain. Moreover, a reduced inclusion of Tau exon 10 has also been reported in a mouse model of DM1 [21]. The CUG expansion sequesters MBNL1, resulting in the mis-splicing of transcripts regulated by this splicing factor. The loss of MBNL1 function can be mimicked using specific siRNAs that target MBNL1 transcripts. Surprisingly, Tau exon 10 splicing is not significantly modulated by a loss of MBNL1 expression, in contrast to Tau exon 2 [19]. The splicing event that we demonstrate here thus appears to be a misregulation induced by long CUG repeats but probably independent of an MBNL1 loss-of-function, as previously suggested for splicing events regulated by CELF1 but not by MBNL1 [30].

3.3. Analysis of CELF proteins: expression and splicing regulation

The present study reports CELF protein expression in DM1 brains. We show that CELF1, CELF2, and CELF4 proteins are expressed in the human brain. Interestingly, an increase in protein levels of CELF1 and CELF2 was observed in the brains of patients DM1a and DM1e but not in the 3 other DM1 patients. GAPDH and CELF4 levels were similar in DM1 and control cases, suggesting that the differences observed were not due to the post mortem delay or the quality of the tissue. Post-translational modifications of splicing factors can modulate their activity. With regard to Tau exon 10 splicing, phosphorylation of the splicing factor hTra21 or SR proteins by the kinases CLK2 or GSK3 promotes the skipping of exon 10 [42–44]. The stability and activity of CELF1 protein is regulated by phosphorylation [30]. Notably, we also observed an increase in CELF1 protein steady-state levels in DM1a and DM1e. CELF1 and CELF2 share more than 70% sequence homology [45] and preliminary data using 2D electrophoresis and Western blotting suggest that CELF2 is also hyperphosphorylated in DM1 brains (data not shown). Therefore, in addition to protein expression, phosphorylation should also be considered to be a modulator of splicing activity in DM1 heart, muscle, and brain.

The splicing of several transcripts (NMDAR1 [20]; cTNT [46]; IR [47]; MTMR1 [48]; and ClC-1 [49]) is modulated by CELF1. However, we found that the overexpression or inactivation of CELF1 does not modulate the splicing of Tau exons 2 and 10. CELF4 promotes Tau exon 2 splicing whereas CELF2 represses it [33]. CELF4 has also been shown to promote Tau exon 10 inclusion [36] but the potential regulation of Tau exon 10 splicing by CELF2 remains unexplored. In this paper, we used HeLa and T98 cells, in which the endogenous expression of CELF4 and CELF2 is lacking [33,50], to show that the ectopic expression of CELF4 promotes Tau exon 10 inclusion whereas CELF2 represses it. Thus, whereas these 3 CELF proteins promote hcTNT exon 5-inclusion, the role of each CELF in Tau splicing was distinct from, and sometimes the opposite of, that of the others, even with respect to a single exon, as reported for α-actinin [51] in non-muscle cells. Therefore, we demonstrate here for the first time that CELF1 has no effect on Tau exons 2 or 10, CELF2 is a repressor of both exons, whereas CELF4 is a repressor of exon 2 and an activator of exon 10 inclusion. Together with other data, we demonstrate that two CELF family splicing factors are strong modulators of Tau splicing [18,33,35]. In addition to these results obtained *in vitro*, we observed a potential relationship between CELF2 overexpression in DM1 and the mis-splicing of Tau exon 10. Since CELF2 levels in DM1b, DM1c, and DM1d were lower than in DM1a and DM1e, and since the former patients showed no change in exon 10, we suggest that Tau exon 10-inclusion is likely related to CELF2 expression or activity in the DM1 brain. It has previously been shown that high levels of CELF2 protein in the forebrain are associated with a skipping of the NMDAR1 NI exon and inclusion of the CI exon and that these splicing patterns are reversed in the hindbrain where CELF2 is deficient [52]. A competitive effect of CELF2 and CELF4 is therefore possible. As CELF2 protein is expressed at higher levels than CELF4 in the brains of DM1a and DM1e, the repressive effect is stronger than the activator effect. In DM1b, c, and d, the disparity between protein levels is not as great and may explain why the promoting effect of CELF4 is in balance with the repressive activity of CELF2.

In conclusion, we show that the altered splicing of Tau exon 10 is likely related to a gain of CELF2 function and neither to a loss of MBNL1 nor a gain of CELF1 functions. Our results strengthen the idea that the CELF proteins are involved in the neuropathology of myotonic dystrophy type I. Noteworthy, CELF2 polymorphisms in combination with Apoliprotein E4 allele are associated with the risk of developping Alzheimer's disease in a recent genome wide association study [60]. Moreover, since neurofibrillary degeneration is a feature common to DM1 patients, particular attention should be paid to cognitive dysfunction related to the temporo-insular brain region.

4. Materials and methods

4.1. DM1 patients and human brain tissue samples

DM1a was a patient followed at the Department of Neurology, Donostia Hospital, San Sebastian, Spain. This patient was a male from the Basque Country in the north of Spain and diagnosed with myotonic dystrophy at the age of 46, with a smear expansion of 333 to 833 CTG triplets as established from blood cells. The initial symptom reported was a cataract operated at the age of 32. In association with typical DM1 symptoms, the patient presented diurnal somnolence, trigeminal neuralgia, and hepatic steatosis. In the last five years, he presented severe proximal weakness that brought him to a wheelchair-bound state. The patient died at 60 years from a disseminated colon neoplasia. DM1e was a woman diagnosed at the age of 46 years old. She presented a myopathic face, suffered from myotonia of both hands, and had type II diabetes, hypercholesterolemia, obesity, and severe restrictive ventilation. Cognitive status was not assessed in either case. Brain tissue samples were obtained at autopsy in accordance with the protocol of the local ethics committee. The other 3 DM1 patients, DM1b, DM1c and DM1d, have been previously described (reference 15 and correspond to case 3, case 1, and case 2, respectively; [19]). These 3 patients were 64, 61, and 53 years old, respectively, at the time of death. Three control individuals were included in the study. Post-mortem delays for tissue sampling were below 48 h. One cerebral hemisphere was frozen and stored at −80 °C and the other was formalin fixed for histological and immunohistochemical studies. Six

cortical brain regions—the temporal, occipital, frontal, entorhinal, and parietal cortices, and the hippocampus—were dissected for analysis. Due to the limited amount of tissue for certain brain regions, such as the hippocampus and entorhinal cortex, biochemical analyses were performed using the temporal, frontal, and parietal cortices. For genetic analysis, all brain regions were included.

4.2. Immunohistochemical analysis

Immunostaining was performed with paraffin-embedded sections. Sections (5 μm-thick) were deparaffinized with xylene and rehydrated through decreasing concentrations of ethanol. Endogenous peroxidase activity was quenched with H_2O_2 and non-specific staining blocked with horse serum using the Vectastain ABC Universal Kit according to the manufacturer's protocol (Vector Laboratories). Brain tissue slices were incubated overnight with the following primary antibodies: AT8, AD2, AT100, S199P, Exon 2, Exon 10, and TauCter. AT8, AT100, Exon 2 (Clone DC 39 1N; Sigma), and Exon 10 (DC 4R; Sigma) are mouse monoclonal antibodies. TauCter and S199P antisera were developed in rabbits against synthetic peptides [15]. AT8 and AT100 label phosphorylated Tau epitopes: AT8 specifically detects phospho-serine 202 and phospho-threonine 205, while AT100 recognizes the pathological phospho-Tau epitopes at serine 212 and threonine 214. Antibodies were diluted 1/100 to 1/1000 in PBS.

4.3. Determination of CTG repeats size and Tau haplotype

Genomic DNA was prepared from brain tissue by phenol–chloroform extraction. The genetic diagnosis of DM1 was confirmed by PCR amplification of the CTG region according to the protocol of Cheng [53], using an Expand Long Template PCR System™ (Roche Diagnostics GmbH, Mannheim, Germany). Each 50 μl reaction consisted of 1× Expand Long PCR Buffer; 0.7 mM each of dATP, dCTP, and dTTP; 0.06 mM dGTP; 0.24 mM 7-deaza dGTP; 1 μM of primers DMK1 (5′-CACAGGCT-GAAGTGGCAGTTCCA-3′) and DMK2 (5′-TGTCGGGGTCTCAGTGCATCCA-3′); 3.5 U of *Taq* DNA polymerase; 1.75 mM $MgCl_2$; and 0.01 to 5 ng of total genomic DNA. Amplifications were performed in a PTC200 thermocycler (MJ Research, Prolabo, France). Following denaturation for 5 min at 95 °C, 35 cycles of amplification were performed: denaturation at 95 °C for 1 min, annealing at 62 °C for 30 s, and extension at 68 °C for 10 min. PCR products were resolved on 1% agarose gels. Southern blot transfer and probe-mediated detection was carried out as follows: agarose gels were denatured in 0.4 M NaOH and 0.6 M NaCl and rinsed twice in 2× SSC before being transferred to Hybond N^+ nylon membranes. Blots were pre-hybridized in DIG Easy Hyb solution (Roche) for 30 min at 59 °C. Hybridization was performed in a fresh solution containing 100 pmol 3′-DIG-$(CTG)_{10}$ (DIG Oligonucleotide Terminal 3′ Labeling Kit; Roche) for 2 h at 59 °C, followed by 2 washes in 2× SSC, 0.1% SDS at room temperature for 5 min, and 2 washes in 0.5× SSC, 0.1% SDS for 15 min at 59 °C. Probe binding was detected using a DIG Luminescence Detection Kit (Roche) according to the manufacturer's instructions (Amersham-Pharmacia Biotech, Orsay, France). Film exposure times ranged from 2 to 5 min. DNA molecular weight standards were loaded onto each agarose gel (DNA Marker IV; Boehringer Mannheim GmbH, Germany). Tau H1/H2 genotyping was performed with primers flanking the 236 bp insertion/deletion polymorphism in intron 9. The forward (5′-GGAAGACGTTCTCACTGATCTG-3′) and reverse (5′-AGGAGTCTGGCTT-CAGTCTCTC-3′) primers used have been previously described [54].

4.4. Semi-quantitative analysis

Total RNA was isolated from brain tissue using RNAgents (Promega, Madison, USA) according to the manufacturer's instructions. Total RNA was isolated from cells using the Nucleospin® RNA II Kit (Macherey Nagel, Düren, Germany). RNA concentration was determined by absorption at 260 nm with NanoDrop ND 1000 Technology (Labtech, France). RT–PCR was performed in triplicate with 1 μg of total RNA using random hexamers (5 μM/l) and M-MLV reverse transcriptase (Invitrogen, CA, USA) according to standard protocols. No DNA amplification was observed in RT controls. PCR was carried out in a final volume of 25 μl, with 10 or 15 pM of each primer (primer sequences are detailed in Supplementary Table 1), 1.5 mM $MgCl_2$, and 1 U of Taq polymerase (Invitrogen), under the following conditions: 5 min at 94 °C, 22 to 30 cycles of a 1 min denaturation step at 94 °C, annealing for 2 min at the temperature indicated in Table 1, 2 min of extension, and 7 min of final extension at 72 °C. 18S was used as an internal control. Reaction products were resolved by electrophoresis using a 4%, 5%, or 8% polyacrylamide gel, and bands were stained with SYBR Gold (Invitrogen). The intensity of SYBR Gold luminescence was measured using a FluoroImager scanner (Claravision, France). The mRNA signals were normalized to that of 18S mRNA.

4.5. Protein extraction and Western blot analysis

DM1 and control brains were homogenized with a Dounce homogenizer in RIPA buffer (Invitrogen, CA, USA) with the addition of 1 mM Na_3VO_4, 125 nM okadaic acid, and protease inhibitors. The resulting homogenates were sonicated and spun at 13,000*g* for 20 min at 4 °C. The supernatants were transferred and the concentration of proteins measured. The pellets were sonicated again, warmed, and centrifuged. The supernatants were diluted with 2× Laemmli Lysis Buffer (LDS Buffer; Invitrogen). The protein extracts (5 μg each) were used for SDS–PAGE (4%–12%; NuPAGE® Bis–Tris Gels; Invitrogen, CA, USA) and transferred onto Hybond nitrocellulose membranes (G&E Healthcare) using the XCell™ II Blot Module (Invitrogen). Proteins were reversibly stained with Ponceau red in order to control for the amount of protein loaded. After blocking with 5% skimmed milk in TBS-T (20 mM Tris–HCl pH 8.0, 150 mM NaCl, and 0.1% Tween-20), membranes were incubated overnight at 4 °C with the following antibodies in the same buffer: anti-CELF1 (Clone 3B1, mouse

Table 1
Clinical, genetic, and neuropathologic characteristics of four DM1 patients.

Case	Age at death	Phenotype class	Intellectual and cognitive status	Neuropathology	Cortical area and size range of the longest (CTG)n expansion
AD	–	Alzheimer's disease	Demented	NFT	–
DM1a	60	Adult form	Not evaluated	NFT	Entorhinal 150–1180
DM1b	64	Adult form	Cognitive impairment	NFT	Temporal 150–3300
DM1c	61	Adult form	Normal	NFT	Temporal 150–2800
DM1d	53	Congenital form	Mental retardation, progressive cognitive impairment	NFT	Temporal 1000–2400
DM1e	61	Adult form	Not evaluated	NFT	Temporal amygdala 140–1820

NFT indicates neurofibrillary tangles.

monoclonal IgG, 1:500; Upstate Biotechnology, Lake Placid, NY, USA), anti-CELF4 (anti-Brunol4, mouse polyclonal, 1:500; Abcam, Cambridge, UK), anti-CELF2 (anti-CUGBP2, mouse monoclonal, 1:1000; Sigma-Aldrich, Saint Louis, MO, USA), and anti-GAPDH as an internal control (anti-FL-335, 1:10,000; Tebu-Bio, Le Perray en Yvelines, France). To label Tau isoforms, we used antibodies specific to exon 2+ (Clone DC 39 1N, 1:1000; Sigma), exon 10+ (DC 4R; Sigma), and Tau exon 10− (anti-Tau 3R-repeat isoform RD3, clone 8E6/C11, 1:1000; Millipore). Membranes were subsequently incubated with a peroxidase-conjugated goat anti-mouse IgG (Sigma-Aldrich; 1:50,000 in the same buffer) or with peroxidase-conjugated goat anti-rabbit IgG (Sigma-Aldrich; 1:4000 in the same buffer), and labeling was revealed using ECL™ and Hyperfilms (G&E, Amersham) according to the manufacturer's instructions. Western blots were carried out at least twice.

4.6. Cell culture and transfection

HeLa cells or T98 glioblastoma cells were grown in monolayer cultures in 6-well plates in Dulbecco's Modified Essential Medium (DMEM) (GIBCO; Invitrogen, CA, USA) supplemented with 10% fetal calf serum, 50 IU/ml penicillin, 50 μg/ml streptomycin, and 4 mmol/l glutamine, at 37 °C in a humidified 5% CO_2 incubator. Cells grown to ~50% confluence were transiently transfected with 1 or 3 μg of plasmid DNA, using FuGENE HD transfection reagent (Roche Diagnostics, IN, USA). Total RNA was analyzed 48 h post-transfection, with 18S RNA as an internal loading standard.

CELF1, CELF4, and CELF2 cDNA in TOPO vectors were sub-cloned using the Gateway System (Invitrogen, France) and inserted into pcDNA3.1/nV5-DEST™ (Invitrogen, France). A V5-epitope was fused to the N-terminal region of CELF factors and their expression was analyzed using both CELF antibodies and a V5-specific antibody (Invitrogen; 1:10,000 dilution). The dominant-negative CELF factor in pcDNA 3.1-His vector (Invitrogen, France) was kindly provided by Thomas Cooper (Baylor College of Medicine, Houston, TX, USA) and corresponds to a CELF4 deletion that has dominant negative activity on itself and other CELF proteins [37]. The protein expression was verified with an Xpress™-specific antibody (Invitrogen) of which epitope is localized at the amino-terminus of the protein. The pcDNA 3.1 empty vector was used as a control. Plasmids containing the 3′ UTR of DMPK with 5 or 200 CTG repeats were derived from previously described constructs under a rodent ROSA promoter controlling GFP fused to the 3′ UTR of *DMPK* [55]. The constructs were sub-cloned into the pcDNA 3.1 vector (Invitrogen, France) under the control of the CMV promoter. The plasmid containing the 3′ UTR of *DMPK* with 960 interrupted CTGs was a minigene vector also under the control of the CMV promoter named DT960. It contained the last 5 exons of the *DMPK* gene followed by the full length *DMPK* 3′ UTR, with 960 CTG repeats interrupted at every 20th repeat by a CTCGA motif [56], named herein CTG960. The conservation of the number of CUG repeats was verified by a long PCR assay. The RTB300-minigene containing exon 5 of human cTNT (hcTNT) has been previously described [57].

For silencing experiments, siRNAs were synthesized by Eurogentec (Belgium). The sense strand sequences of the siRNAs designed to target MBNL1 mRNA transcripts were siMBNL1a 5′-CGCAGUUGGAGAUAAAUGG-3′ and siMBNL1b 5′-CAGACAGACUUGAGGUAUG-3′ [58]. To target CELF1 mRNA transcripts, the sense strand sequences of the siRNAs were siCELF1a 5′-GUUACGACAAUCCUGUUUCdTdT-3′ (described by Paul et al. [59]) and siCELF1b 5′-CACCCGUAAAGCUGCAUUdTdT-3′. Scrambled siRNAs and siRNA against β-actin were also designed as controls. The siRNAs were transfected using Oligofectamine Reagent (Invitrogen) according to the manufacturer's instructions. Increasing concentrations were used (10, 50, 100, and 200 nM) to determine the dose–response curve; otherwise, siRNA concentration used was 100 nM.

4.7. Statistical analysis

Statistical analyses were performed using the non-parametric Mann–Whitney test or one-way ANOVA, using Prism Software (GraphPad Software Inc., San Diego, CA, USA).

Supplementary materials related to this article can be found online at doi: 10.1016/j.bbadis.2011.03.010.

Acknowledgments

We thank the AFM, the INSERM, and the University Lille Nord de France. We would like to dedicate this study to DM1 patients who directly contributed to important breakthroughs regarding DM1 pathophysiology by giving their bodies to science. We are grateful to Thomas Cooper (Department of Pathology and Immunology, Department of Molecular and Cellular Biology, Baylor College of Medicine, Houston, TX 77030, USA) for providing us with the DT960, CTG960, and dominant-negative CELF plasmids, as well as Mani S. Mahadevan (Department of Pathology, University of Virginia, Charlottesville, VA 22908, USA) for providing us the pROSA-GFP-3′ UTR *DMPK* CTG5 and CTG200 constructs. Funding: MG, AS, and ALM received funding from the Instituto de la Salud Carlos III, Ministerio de Educación, Ilundain Fundazioa, and CIBERNED.

Disclosure: The authors have no conflict of interest to report.

References

[1] P.S. Harper, Myotonic Dystrophy, WB Saunders, London, 2001.
[2] W.J. Adie, J.G. Greenfield, Dystrophia myotonica (myotonia atrophica), Brain 46 (1923) 73–127.
[3] R. Gibson, Dystrophia myotonica in association with mental defect, Can. Med. Assoc. J. 84 (1961) 1234–1237.
[4] P. Malloy, S.K. Mishra, S.H. Adler, Neuropsychological deficits in myotonic muscular dystrophy, J. Neurol. Neurosurg. Psychiatry 53 (1990) 1011–1013.
[5] S. Winblad, P. Hellstrom, C. Lindberg, S. Hansen, Facial emotion recognition in myotonic dystrophy type 1 correlates with CTG repeat expansion, J. Neurol. Neurosurg. Psychiatry 77 (2006) 219–223.
[6] S. Winblad, C. Lindberg, S. Hansen, Cognitive deficits and CTG repeat expansion size in classical myotonic dystrophy type 1 (DM1), Behav. Brain Funct. 2 (2006) 16.
[7] A. Sistiaga, I. Urreta, M. Jodar, A.M. Cobo, J. Emparanza, D. Otaegui, J.J. Poza, J.J. Merino, H. Imaz, J.F. Marti-Masso, A. Lopez de Munain, Cognitive/personality pattern and triplet expansion size in adult myotonic dystrophy type 1 (DM1): CTG repeats, cognition and personality in DM1, Psychol. Med. (2009) 1–9.
[8] V. Sansone, S. Gandossini, M. Cotelli, M. Calabria, O. Zanetti, G. Meola, Cognitive impairment in adult myotonic dystrophies: a longitudinal study, Neurol. Sci. 28 (2007) 9–15.
[9] G. Meola, V. Sansone, Cerebral involvement in myotonic dystrophies, Muscle Nerve 36 (2007) 294–306.
[10] S. Winblad, J.E. Mansson, K. Blennow, C. Jensen, L. Samuelsson, C. Lindberg, Cerebrospinal fluid tau and amyloid beta42 protein in patients with myotonic dystrophy type 1, Eur. J. Neurol. 15 (2008) 947–952.
[11] C. Kornblum, J. Reul, W. Kress, C. Grothe, N. Amanatidis, T. Klockgether, R. Schroder, Cranial magnetic resonance imaging in genetically proven myotonic dystrophy type 1 and 2, J. Neurol. 251 (2004) 710–714.
[12] A. Di Costanzo, F. Di Salle, L. Santoro, A. Tessitore, V. Bonavita, G. Tedeschi, Pattern and significance of white matter abnormalities in myotonic dystrophy type 1: an MRI study, J. Neurol. 249 (2002) 1175–1182.
[13] A. Di Costanzo, F. Di Salle, L. Santoro, V. Bonavita, G. Tedeschi, Brain MRI features of congenital- and adult-form myotonic dystrophy type 1: case–control study, Neuromuscul. Disord. 12 (2002) 476–483.
[14] P. Vermersch, N. Sergeant, M.M. Ruchoux, H. Hofmann-Radvanyi, A. Wattez, H. Petit, P. Dwailly, A. Delacourte, Specific tau variants in the brains of patients with myotonic dystrophy, Neurology 47 (1996) 711–717.
[15] N. Sergeant, B. Sablonniere, S. Schraen-Maschke, A. Ghestem, C.A. Maurage, A. Wattez, P. Vermersch, A. Delacourte, Dysregulation of human brain microtubule-associated tau mRNA maturation in myotonic dystrophy type 1, Hum. Mol. Genet. 10 (2001) 2143–2155.
[16] C.A. Maurage, B. Udd, M.M. Ruchoux, P. Vermersch, H. Kalimo, R. Krahe, A. Delacourte, N. Sergeant, Similar brain tau pathology in DM2/PROMM and DM1/Steinert disease, Neurology 65 (2005) 1636–1638.
[17] N. Sergeant, A. Bretteville, M. Hamdane, M.L. Caillet-Boudin, P. Grognet, S. Bombois, D. Blum, A. Delacourte, F. Pasquier, E. Vanmechelen, S. Schraen-Maschke, L. Buee, Biochemistry of Tau in Alzheimer's disease and related neurological disorders, Expert Rev. Proteomics 5 (2008) 207–224.
[18] A. Andreadis, Tau gene alternative splicing: expression patterns, regulation and modulation of function in normal brain and neurodegenerative diseases, Biochim. Biophys. Acta 1739 (2005) 91–103.
[19] C.M. Dhaenens, S. Schraen-Maschke, H. Tran, V. Vingtdeux, D. Ghanem, O. Leroy, J. Delplanque, E. Vanbrussel, A. Delacourte, P. Vermersch, C.A. Maurage, H. Gruffat,

A. Sergeant, M.S. Mahadevan, S. Ishiura, L. Buee, T.A. Cooper, M.L. Caillet-Boudin, N. Charlet-Berguerand, B. Sablonniere, N. Sergeant, Overexpression of MBNL1 fetal isoforms and modified splicing of Tau in the DM1 brain: two individual consequences of CUG trinucleotide repeats, Exp. Neurol. 210 (2008) 467–478.
[20] H. Jiang, A. Mankodi, M.S. Swanson, R.T. Moxley, C.A. Thornton, Myotonic dystrophy type 1 is associated with nuclear foci of mutant RNA, sequestration of muscleblind proteins and deregulated alternative splicing in neurons, Hum. Mol. Genet. 13 (2004) 3079–3088.
[21] M. Gomes-Pereira, L. Foiry, A. Nicole, A. Huguet, C. Junien, A. Munnich, G. Gourdon, CTG trinucleotide repeat "big jumps": large expansions, small mice, PLoS Genet. 3 (2007) e52.
[22] R. Dixit, J.L. Ross, Y.E. Goldman, E.L. Holzbaur, Differential regulation of dynein and kinesin motor proteins by tau, Science 319 (2008) 1086–1089.
[23] L.M. Ittner, Y.D. Ke, F. Delerue, M. Bi, A. Gladbach, J. van Eersel, H. Wolfing, B.C. Chieng, M.J. Christie, I.A. Napier, A. Eckert, M. Staufenbiel, E. Hardeman, J. Gotz, Dendritic function of tau mediates amyloid-beta toxicity in Alzheimer's disease mouse models, Cell 142 (2010) 387–397.
[24] B.R. Hoover, M.N. Reed, J. Su, R.D. Penrod, L.A. Kotilinek, M.K. Grant, R. Pitstick, G.A. Carlson, L.M. Lanier, L.L. Yuan, K.H. Ashe, D. Liao, Tau mislocalization to dendritic spines mediates synaptic dysfunction independently of neurodegeneration, Neuron 68 (2010) 1067–1081.
[25] J.D. Brook, M.E. McCurrach, H.G. Harley, A.J. Buckler, D. Church, H. Aburatani, K. Hunter, V.P. Stanton, J.P. Thirion, T. Hudson, et al., Molecular basis of myotonic dystrophy: expansion of a trinucleotide (CTG) repeat at the 3′ end of a transcript encoding a protein kinase family member, Cell 69 (1992) 385.
[26] R.N. Kanadia, K.A. Johnstone, A. Mankodi, C. Lungu, C.A. Thornton, D. Esson, A.M. Timmers, W.W. Hauswirth, M.S. Swanson, A muscleblind knockout model for myotonic dystrophy, Science 302 (2003) 1978–1980.
[27] N.M. Kuyumcu-Martinez, T.A. Cooper, Misregulation of alternative splicing causes pathogenesis in myotonic dystrophy, Prog. Mol. Subcell. Biol. 44 (2006) 133–159.
[28] N.A. Timchenko, Z.J. Cai, A.L. Welm, S. Reddy, T. Ashizawa, L.T. Timchenko, RNA CUG repeats sequester CUGBP1 and alter protein levels and activity of CUGBP1, J. Biol. Chem. 276 (2001) 7820–7826.
[29] J.P. Orengo, P. Chambon, D. Metzger, D.R. Mosier, G.J. Snipes, T.A. Cooper, Expanded CTG repeats within the DMPK 3′ UTR causes severe skeletal muscle wasting in an inducible mouse model for myotonic dystrophy, Proc. Natl Acad. Sci. U.S.A. 105 (2008) 2646–2651.
[30] N.M. Kuyumcu-Martinez, G.S. Wang, T.A. Cooper, Increased steady-state levels of CUGBP1 in myotonic dystrophy 1 are due to PKC-mediated hyperphosphorylation, Mol. Cell 28 (2007) 68–78.
[31] A.N. Ladd, N. Charlet, T.A. Cooper, The CELF family of RNA binding proteins is implicated in cell-specific and developmentally regulated alternative splicing, Mol. Cell. Biol. 21 (2001) 1285–1296.
[32] A.N. Ladd, N.H. Nguyen, K. Malhotra, T.A. Cooper, CELF6, a member of the CELF family of RNA-binding proteins, regulates muscle-specific splicing enhancer-dependent alternative splicing, J. Biol. Chem. 279 (2004) 17756–17764.
[33] O. Leroy, C.M. Dhaenens, S. Schraen-Maschke, K. Belarbi, A. Delacourte, A. Andreadis, B. Sablonniere, L. Buee, N. Sergeant, M.L. Caillet-Boudin, ETR-3 represses Tau exons 2/3 inclusion, a splicing event abnormally enhanced in myotonic dystrophy type I, J. Neurosci. Res. 84 (2006) 852–859.
[34] T.M. Caffrey, C. Joachim, S. Paracchini, M.M. Esiri, R. Wade-Martins, Haplotype-specific expression of exon 10 at the human MAPT locus, Hum. Mol. Genet. 15 (2006) 3529–3537.
[35] J.P. Chapple, K. Anthony, T.R. Martin, A. Dev, T.A. Cooper, J.M. Gallo, Expression, localization and tau exon 10 splicing activity of the brain RNA-binding protein TNRC4, Hum. Mol. Genet. 16 (2007) 2760–2769.
[36] J. Wang, Q.S. Gao, Y. Wang, R. Lafyatis, S. Stamm, A. Andreadis, Tau exon 10, whose missplicing causes frontotemporal dementia, is regulated by an intricate interplay of cis elements and trans factors, J. Neurochem. 88 (2004) 1078–1090.
[37] G. Singh, B.N. Charlet, J. Han, T.A. Cooper, ETR-3 and CELF4 protein domains required for RNA binding and splicing activity in vivo, Nucleic Acids Res. 32 (2004) 1232–1241.
[38] M. Kobayakawa, N. Tsuruya, A. Takeda, A. Suzuki, M. Kawamura, Facial emotion recognition and cerebral white matter lesions in myotonic dystrophy type 1, J. Neurol. Sci. 290 (2010) 48–51.
[39] A. Delacourte, N. Sergeant, A. Wattez, D. Gauvreau, Y. Robitaille, Vulnerable neuronal subsets in Alzheimer's and Pick's disease are distinguished by their tau isoform distribution and phosphorylation, Ann. Neurol. 43 (1998) 193–204.
[40] C. Mailliot, N. Sergeant, T. Bussiere, M.L. Caillet-Boudin, A. Delacourte, L. Buee, Phosphorylation of specific sets of tau isoforms reflects different neurofibrillary degeneration processes, FEBS Lett. 433 (1998) 201–204.
[41] Q.S. Gao, J. Memmott, R. Lafyatis, S. Stamm, G. Screaton, A. Andreadis, Complex regulation of tau exon 10, whose missplicing causes frontotemporal dementia, J. Neurochem. 74 (2000) 490–500.
[42] A.M. Hartmann, D. Rujescu, T. Giannakouros, E. Nikolakaki, M. Goedert, E.M. Mandelkow, Q.S. Gao, A. Andreadis, S. Stamm, Regulation of alternative splicing of human tau exon 10 by phosphorylation of splicing factors, Mol. Cell. Neurosci. 18 (2001) 80–90.
[43] D.C. Glatz, D. Rujescu, Y. Tang, F.J. Berendt, A.M. Hartmann, F. Faltraco, C. Rosenberg, C. Hulette, K. Jellinger, H. Hampel, P. Riederer, H.J. Moller, A. Andreadis, K. Henkel, S. Stamm, The alternative splicing of tau exon 10 and its regulatory proteins CLK2 and TRA2-BETA1 changes in sporadic Alzheimer's disease, J. Neurochem. 96 (2006) 635–644.
[44] F. Hernandez, M. Perez, J.J. Lucas, A.M. Mata, R. Bhat, J. Avila, Glycogen synthase kinase-3 plays a crucial role in tau exon 10 splicing and intranuclear distribution of SC35. Implications for Alzheimer's disease, J. Biol. Chem. 279 (2004) 3801–3806.
[45] C. Barreau, L. Paillard, A. Mereau, H.B. Osborne, Mammalian CELF/Bruno-like RNA-binding proteins: molecular characteristics and biological functions, Biochimie 88 (2006) 515–525.
[46] A.V. Philips, L.T. Timchenko, T.A. Cooper, Disruption of splicing regulated by a CUG-binding protein in myotonic dystrophy, Science 280 (1998) 737–741.
[47] R.S. Savkur, A.V. Philips, T.A. Cooper, Aberrant regulation of insulin receptor alternative splicing is associated with insulin resistance in myotonic dystrophy, Nat. Genet. 29 (2001) 40–47.
[48] A. Buj-Bello, D. Furling, H. Tronchere, J. Laporte, T. Lerouge, G.S. Butler-Browne, J.L. Mandel, Muscle-specific alternative splicing of myotubularin-related 1 gene is impaired in DM1 muscle cells, Hum. Mol. Genet. 11 (2002) 2297–2307.
[49] B.N. Charlet, R.S. Savkur, G. Singh, A.V. Philips, E.A. Grice, T.A. Cooper, Loss of the muscle-specific chloride channel in type 1 myotonic dystrophy due to misregulated alternative splicing, Mol. Cell 10 (2002) 45–53.
[50] V.A. Barron, H. Zhu, M.N. Hinman, A.N. Ladd, H. Lou, The neurofibromatosis type I pre-mRNA is a novel target of CELF protein-mediated splicing regulation, Nucleic Acids Res. (2009).
[51] N. Gromak, A.J. Matlin, T.A. Cooper, C.W. Smith, Antagonistic regulation of alpha-actinin alternative splicing by CELF proteins and polypyrimidine tract binding protein, RNA 9 (2003) 443–456.
[52] W. Zhang, H. Liu, K. Han, P.J. Grabowski, Region-specific alternative splicing in the nervous system: implications for regulation by the RNA-binding protein NAPOR, RNA 8 (2002) 671–685.
[53] S. Cheng, J.M. Barcelo, R.G. Korneluk, Characterization of large CTG repeat expansions in myotonic dystrophy alleles using PCR, Hum. Mutat. 7 (1996) 304–310.
[54] M. Baker, I. Litvan, H. Houlden, J. Adamson, D. Dickson, J. Perez-Tur, J. Hardy, T. Lynch, E. Bigio, M. Hutton, Association of an extended haplotype in the tau gene with progressive supranuclear palsy, Hum. Mol. Genet. 8 (1999) 711–715.
[55] J.D. Amack, A.P. Paguio, M.S. Mahadevan, Cis and trans effects of the myotonic dystrophy (DM) mutation in a cell culture model, Hum. Mol. Genet. 8 (1999) 1975–1984.
[56] T.H. Ho, R.S. Savkur, M.G. Poulos, M.A. Mancini, M.S. Swanson, T.A. Cooper, Colocalization of muscleblind with RNA foci is separable from mis-regulation of alternative splicing in myotonic dystrophy, J. Cell Sci. 118 (2005) 2923–2933.
[57] T.A. Cooper, Muscle-specific splicing of a heterologous exon mediated by a single muscle-specific splicing enhancer from the cardiac troponin T gene, Mol. Cell. Biol. 18 (1998) 4519–4525.
[58] T.H. Ho, B.N. Charlet, M.G. Poulos, G. Singh, M.S. Swanson, T.A. Cooper, Muscleblind proteins regulate alternative splicing, EMBO J. 23 (2004) 3103–3112.
[59] S. Paul, W. Dansithong, D. Kim, J. Rossi, N.J. Webster, L. Comai, S. Reddy, Interaction of muscleblind, CUG-BP1 and hnRNP H proteins in DM1-associated aberrant IR splicing, EMBO J 25 (2006) 4271–4283.
[60] E.M. Wijsman, N.D. Pankratz, Y. Choi, J.H. Rothstein, K.M. Faber, R. Cheng, J.H. Lee, T.D. Bird, D.A. Bennett, R. Diaz-Arrastia, A.M. Goate, M. Farlow, B. Ghetti, R.A. Sweet, T.M. Foroud, R. Mayeux, Genome-Wide Association of Familial Late-Onset Alzheimer's Disease Replicates BIN1 and CLU and Nominates CUGBP2 in Interaction with APOE, PLoS Genet 7, e1001308.